

The influence of the static field on the motion stability of a hexapole rf trap

C. M. NICULAE*, M. NICULAE

Faculty of Physics, University of Bucharest, Bucharest-Magurele P.O. Box MG11, 077125, Romania

The stability of hexapole rf trap under DC electric field is theoretically investigated. Analytical arguments based on the 3D slow-fast Kapitsa method are developed to find the locus of the minimum in the effective potential. We investigate the motions with both vanishing and not vanishing angular momentum with respect to the z-axis. The numerical analysis confirms the theoretical results.

(Received May 18, 2009; accepted September 30, 2009)

Keywords: Multipole rf traps, Nonlinear dynamics, Nonlinear systems

1. Introduction

Today, half a century after the invention of the quadrupole radiofrequency (rf) trap, also known as the Paul trap [1], and approximately seven decades after the invention of the Penning trap [2], ion traps are far from becoming obsolete. Such longevity is largely due to their ability to confine charged particles to small volumes in well controlled fields. Such traps are highly sensitive devices since they allow single ions to be stored and detected. Ions confinement for long periods of time is the key to high precision in particular if frequencies are to be measured. In our days, ion traps are used in analytical chemistry, trace analysis, molecular and cluster physics, the physics of non-neutral plasmas, metrology, atomic spectroscopy, high-precision mass spectrometry on stable or unstable isotopes, and for ion beam manipulation.

Over the past two decades, higher order radiofrequency traps (like octupole [3] or hexapole [4]), unusual designs of the Paul trap [5], linear traps [6], and other electrode setups whose potential contains two or more multipole terms, have been intensively investigated in order to design charged-particle traps for high precision spectroscopy, frequency standards and for investigations in quantum optics [7].

The motion stability problem for the rf traps is the key problem of such a research. In a Paul trap the motion of the particle is described by linear, uncoupled, and explicitly time-dependent equations of motion (Mathieu equations). While for such traps the Floquet theory completely solves the stability problem for, in the case of higher order rf traps the stability problem is far from being solved. The reason of this state of facts resides in the natural complexity of such problems. The involved equations of motions are nonlinear, non-autonomous, spatial, and temporally coupled. Specifically, the temporal coupling appears from their common dependence on time. This coupling is scarcely, or even not at all discussed in literature. In the case of 2D motions in a Paul trap for instance, the coupling is responsible for the specific form

(a rectangle with missing corners) of the outer boundary of the area covered by the particle motion.

There are many attempts to overcome these difficulties. Most of them are based on both experimental and theoretical arguments. In this area there are only few contributions that help understanding the relevant features of such motions. One of them refers to the so called *adiabatic approximation* [4, 8]. In the rf trap domain, the adiabatic approximation is based on an older method, first introduced by Kapitsa [9]. This method allows the determination of the effective potential function that gives a hint about the reason of why such devices can confine charged particles. When the effective potential is derived only from the AC component of the driving field, it is called *pseudopotential* function [8]. It also allows the introduction of two major terms: *macro-* and *micromotion*, respectively. In this model, a charged particle, moving into a non-uniform, rapidly time-varying field, experiences a net force whose direction is toward regions of weaker field.

Its trajectory can be thought of as being the superposition of two motions: one of large amplitude and low frequency as compared to the frequency of the driving field - *macromotion* (also called *secular* motion), and another one of small amplitude and synchronous to the driving field - the *micromotion*.

The effective potential function is useful in determining the direction of this net force. When designing new rf traps, or new ion guides, the pseudopotential function is a very useful instrument to find, even in the incipient stage of trap design, if the electrode setup is able, or not, to accommodate confined motions. To understand the known features described below when characterizing the single ion motion into a nonlinear rf trap, some concepts in the domain are defined. For all rf (2n-pole) traps it is useful to define a parameter q_n that is proportional to $eV/(m\Omega^2 a^2)$, where a is a representative dimension for the trap (customarily, half the inner distance between endcaps), Ω and V represent the

frequency and the amplitude of the driving field, while m and e are the mass and the charge of the ion, respectively.

A list of some known facts, or generally accepted features concerning the motion stability in rf traps, is given below:

(i) Though there is no theoretical proof yet, the existence of stable motions has been generally accepted in vicinity of the trap center [4, 10].

(ii) Generally, the larger the kinetic energy of an ion, the larger the spatial region covered by its motion. This is not true for motions that occupy different regions of the trap. For instance, two ions launched from the center of a hexapole rf trap, with the same kinetic energy, the first one along the z -axis and the second one along the $x = 2z$ line, have distinct ratio of their amplitudes. The elongation of the ion motion in the second case is larger.

(iii) The maximum kinetic energy of the stable motions decreases with q_n [3, 4].

(iv) For given kinetic energy, the dimensions of the region covered by stable motions decreases with q_n [4].

(v) Excepting some particular periodic motions, the single ion 3D motion exhibits chaotic dynamics. This is also true even for simple motions like rectilinear motions.

(vi) Generally, the chaotic feature is not related to the spatial stability, since chaotic stable motions also exist.

To our knowledge, the influence of the DC component on the dynamics in higher-order rf trap has been scarcely studied so far. The only available information states that, unlike the behavior in a Paul trap, *in the octupole rf trap the presence of a DC potential is generally proved to deteriorate the trap stability* [3].

2. The hexapole rf trap

A hexapole rf trap is an electronic device whose confining potential is shaped by four electrodes having axial symmetry: two rings and two endcaps (Fig. 1).

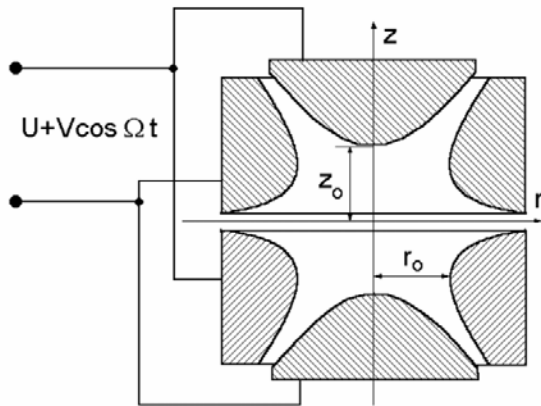


Fig.1. Electrode structure of the hexapole rf trap.

The ideal potential that this electrode geometry has to approach is given by

$$\Phi(x, y, z) = \Phi_0 (2z^2 - 3x^2 - 3y^2)z / 4z_0^3 \quad (1)$$

Generally, the electrode design of a $2n$ -order rf trap should approximate the three-dimensional potential [3, 4].

$$\Phi(r, \theta, \varphi) = A \Phi_n^{(n)}(\cos \theta) \quad (2)$$

where (r, θ, φ) denote the usual spherical coordinates and $\Phi_n^{(n)}$ is the Legendre polynomial of n order. Customarily, the ideal surfaces of the electrodes can be determined by solving the equations

$$\Phi(r, \theta, \varphi) = \pm \Phi_0 / 2 \quad (3)$$

In the hexapole rf trap case, the design constrains (3) introduces a relation between the minimum radius of the ring electrode r_0 and the half of the inner distance between endcaps z_0 expressed by $r_0 = z_0 / \sqrt{2}$. Such a device becomes a rf trap when Φ_0 includes a radiofrequency component which can be written as

$$\Phi_0(z) = U + V \cos(\Omega t) \quad (4)$$

where U , V , and $\Omega/2\pi$ denote the DC, AC voltages applied between adjacent electrodes, and the driving frequency, respectively.

The equations describing the motion of a particle of mass m and charge e into a hexapole rf trap read

$$\begin{aligned} d^2x/dt^2 &= 2\pi z A \\ d^2y/dt^2 &= 2\pi z A \\ d^2z/dt^2 &= (x^2 + y^2 - 2z^2)A \end{aligned} \quad (5)$$

where $A = 3e\Phi_0(z)/(4mz_0^3)$. One of the simplest forms of the equations of motion is given by

$$\begin{aligned} d^2\xi/d\tau^2 &= \xi\xi(\sigma + \cos\tau) \\ d^2\eta/d\tau^2 &= \eta\eta(\sigma + \cos\tau) \\ d^2z/d\tau^2 &= (\xi^2 + \eta^2 - 2z^2)(\sigma + \cos\tau)/2 \end{aligned} \quad (6)$$

where the new spatial coordinates are related to the old ones by $[\xi \eta z] = (3/4)q_z[x y z]/z_0$, and the time-scale is chosen such as $\Omega t = \tau$. The parameter σ represents the ratio U/V of the DC to AC components of the confining electric field $U + V \cos(\Omega t)$, while the parameter $q_z = 2eV/(m\Omega^2 z_0^3)$ is the q parameter of the Mathieu equation governing the motion along the z axis in a Paul trap.

Of course, the new form preserves all the information about the motion stability in a hexapole trap [4]. Notice that an ion belongs to the inner space of the trap if $|2z^2 - 3z(x^2 + y^2)| \leq 2z_0^3$ [which, in our dimensionless variables, reads as $|2z^2 - 3z(\xi^2 + \eta^2)| \leq (27/32)q_z^2$].

It should be noted here that equation (6) reveals a single parameter, σ , through which particle motion can be controlled. Therefore σ becomes the only parameter by which we can influence the stability of motion in the hexapole rf trap.

Aside from this parameter, the initial conditions only remain to determine the stability of the motion, this feature being characteristic to all nonlinear rf trap.

3. The effective potential derived by Kapitsa method

This method, also known as *adiabatic approximation*, originally proposed by Kapitsa [9], and developed by Landau [11], Dehmelt [8], and others, assumes that the motion of the particle might be decomposed into a slow component (X, Y, Z) having a large amplitude and low frequency as compared to the fast motion (u, v, w) driven by the rf field. In mathematical form, this means

$$\dot{z} = X + u, \dot{y} = Y + v, \dot{x} = Z + w, \quad (7)$$

The fast motion is considered as having a zero average over a period of the driving voltage, that is $\bar{u} = \bar{v} = \bar{w} = 0$. More precisely, in this paper we used the running average $\bar{f} = (1/T) \int_0^T f(t) dt$, where T represents the period over which the average is done.

For the sake of generality, we used the *slow* and *fast* terms, instead of the corresponding Dehmelt terms, *macromotion* and *micromotion*, widely used in the rf trap literature.

Following the Kapitsa method, the following equations for the slow motion are derived

$$\begin{aligned} \dot{X} &= \alpha X Z - X(X^2 + Y^2)/4, \\ \dot{Y} &= \alpha Y Z - Y(X^2 + Y^2)/4, \\ \dot{Z} &= \alpha(X^2 + Y^2 - 2Z^2)/2 - Z^3, \end{aligned} \quad (8)$$

It is easy to notice that (8) could be rewritten in a more compact form

$$\dot{\mathcal{S}} = -\nabla \mathcal{W}_0 - \nabla \mathcal{W}_1 \quad (9)$$

where $\mathcal{S} = (X, Y, Z)$. The *dynamic potential* $\mathcal{W}_0(\mathcal{S}) = Z^2/4 + (X^2 + Y^2)^2/16$ represents the dimensionless form of the Dehmelt pseudopotential, while the potential function $\mathcal{W}_1(\mathcal{S}) = \alpha [2Z^3 - 3Z(X^2 + Y^2)]/4$ corresponds to the *static potential* of the hexapole trap. Indeed, the pseudopotential function of a multipole rf trap is, by definition, [3, 8].

$$\mathcal{W}_2(\mathcal{S}) = \frac{e}{4m\alpha c^2} [\mathcal{S}(\mathcal{S})]^2 \quad (10)$$

which, in the case of the hexapole rf trap, becomes

$$\mathcal{W}_2(\mathcal{S}) = 32V/(9q_2^2) \mathcal{W}_0(\mathcal{S}) \quad (11)$$

On the other hand, the static potential of the hexapole trap could be written as

$$\mathcal{W}_3(\mathcal{S}) = 32V/(9q_2^2) \mathcal{W}_1(\mathcal{S}) \quad (12)$$

It is interesting to notice that the effective potential function $\mathcal{W} = \mathcal{W}_0 + \mathcal{W}_1$ has an absolute minimum on a circle of radius $2|c|$ that belongs to the $Z = c$ plane, a relative minimum on the z-axis at $Z = -c$, and a minimax

at the origin. If we express \mathcal{W} in (R, Z) coordinates it is easy to see that $\mathcal{W}(2|c|, c) = -3c^4/12$ at the absolute minimum, and $\mathcal{W}(0, -c) = -c^4/12$ at the relative minimum.

In the real space, this means that when including the DC component, the confinement center moves from origin either to a point belonging to a circle of radius $8\alpha_0|c|/3q_2$ from the plane $z = 4\alpha_0|c|/3q_2$, or to the point $z = -4\alpha_0|c|/3q_2$ on the z-axis. It should be emphasized that this circle belongs to the conic $x^2 + y^2 = 4z^2$ that is the same conic in which rectilinear trajectories are possible in the hexapole trap [4]. Likewise, the relative minimum belongs to the z-axis on which rectilinear motions are also possible.

One can imagine the trap center as a mountain pass between three valleys. The bottom of the upper valley lies on the z-axis, while the deeper ones extend along the $x = \pm 2z$ lines.

A similar analysis shows that in the case of the octupole trap the confinement center splits into two circles, one above and the second one below the $z = 0$ plane. We did not fail to notice that this splitting (in the octupole case) could cause the deterioration of the trap stability as the experiment showed [3].

4. Motion stability for rectilinear motions

The existence of these rectilinear motions in the 2n-pole traps have been proven in [4, 12]. In a plane passing through the symmetry axis, there are n such motions, one of them being the axis itself. Their study is important for the following reasons: a) all these motions are described by the same equation; b) the minima of the effective potential for 2D motions belong to the locus of these rectilinear motions; c) the most distanced point from the trap center of all motions with the same average kinetic energy, measured in the vicinity of the trap center, belongs to, or is approximately one of the rectilinear motions.

Theoretical predictions. In this section we focus on the rectilinear motion along the z-axis only given by

$$d^2z/dt^2 = -z^2(\alpha + \cos z) \quad (13)$$

in dimensionless coordinates.

For this motion the equation of the slow motion reads

$$d^2Z/dt^2 = -Z^3 - \alpha Z^4 \quad (14)$$

Any numerical analysis should be verified before we can trust it. To this end, in the classical physics involved here, it is a good idea to look for some invariants. Fortunately, this motion has some (the well-known one – the projection on the z-axis of the angular momentum – is useless for rectilinear motions), but only for the slow motion introduced by the adiabatic approximation:

(1) For $\alpha = 0$, the product of the amplitude A and the period T of the slow motion is conserved

$$AT = 7.410298 \dots \quad (15)$$

The fact that the product satisfies $AT = \text{constant}$ is a direct consequence of the similitude principle [11]. This principle applies to cases where the force is derived from homogeneous potentials. A hint about how this principle works is given below. Let there be two distinct motions described by

$$d^2Z/d\tau^2 = -Z^3 \quad (16)$$

Let there A_1, A_2 be their amplitudes and T_1, T_2 be their periods, respectively. Let us consider a change of the variables $Z = A_1 S, \tau = t/A_1$ for the first one, and $Z = A_2 S, \tau = t/A_2$ for the second one. In the new coordinates, the first motion has an amplitude $S_1 = 1$ and a period $A_1 T_1$, while the amplitude and the period of the second one are $S_2=1$ and $A_2 T_2$, respectively. Now, the two motions are described by the same equation $d^2S/d\tau^2 = -S^3$, and since they have the same amplitude, in fact, we deal with a unique motion. Consequently, the two periods should be equal: $A_1 T_1 = A_2 T_2$. As the two amplitudes or periods are arbitrarily chosen, it follows that generally $AT = \text{constant}$ (QED). The number in equation (15) approximates the period of a motion whose amplitude is 1. Indeed $AT = 1 \cdot T_1 = \text{constant}$. The period T_1 might be computed by integrating twice equation (16). A formula that speculates the symmetry of this motion and allows the evaluation of this invariant is

$$T_1 = 4\sqrt{2} \int_0^1 \frac{dz}{\sqrt{1-z^4}} = 7.410298 \dots \quad (17)$$

(2) Another invariant of equation (14) is

$$Z^4 + \frac{Z^6}{\epsilon} + \frac{6\epsilon Z^8}{\epsilon} = \text{constant} = 2H \quad (18)$$

where H may acquire the significance of total energy in our dimensionless coordinates.

Denoting the lower, upper positions with Z_{\min}, Z_{\max} , and maximum velocity of the slow motion with Z_{max} , the $2H$ constant could be rewritten as

$$\frac{Z_{\min}^4}{\epsilon} + \frac{6\epsilon Z_{\min}^8}{\epsilon} = \frac{Z_{\max}^4}{\epsilon} + \frac{6\epsilon Z_{\max}^8}{\epsilon} = Z_{\text{max}}^4 - \frac{\epsilon^4}{\epsilon} \quad (19)$$

The energetic invariant in Eq. (19) can then be generalized to the 3D case

$$H = H + \Psi = K_{\text{tot}} - \frac{K^4}{12} = K_{\text{rel}} - \frac{\epsilon^4}{12} \quad (20)$$

where K is the kinetic energy $(X^2 + Y^2 + Z^2)/2$, K_{tot} is the kinetic energy that can be reduced to zero when the particle lies at the bottom of the absolute minimum of Ψ , and K_{rel} is kinetic energy that can be reduced to zero when the particle lies at the bottom of the relative minimum of Ψ . Since in this section we deal with the motion along the z -axis, the minimum of the Ψ in this case is $-\epsilon^4/12$. This

explains the term $-\epsilon^4/6$ in the right hand side of equation (19).

Generally, for all values of ϵ , the period of the slow motion can be obtained by integrating equation (14) twice

$$T = 2 \int_{Z_{\min}}^{Z_{\max}} \frac{dz}{\sqrt{2H - Z^4 - 6\epsilon Z^8}} \quad (21)$$

where $f(\epsilon) = \epsilon^4/2 + 2\epsilon\epsilon^2/3$, and $T = 2\pi/\omega_z$. The relative angular frequency ω_z is defined as the ratio $\omega_{\text{slow}}/\Omega$ of the secular frequency ω_{slow} to the driving frequency Ω .

Notice that T depends on ϵ and Z_{\max} only, since the limits of the integral depend on these parameters. Indeed, for any values of the pair (ϵ, Z_{\max}) , equation (18) has only two real roots: Z_{\min} and Z_{\max} .

5. Numeric results for rectilinear motion

The goal of this section is to find how far we can trust the adiabatic approximation. In this sense, we asked the following question: If it is good, to what extent is it good? If it is wrong, why, and where does it fail? Historically, this study comes last being imposed by some failures of the adiabatic approximation noticed in the 2D and 3D analyses. The most important seems to be a shift of the positions of the extrema of the effective potential from the predicted position toward the exterior of the trap. Anticipating, this shift increases with ϵ . Another feature that could be important for applications is the non-monotonic dependence of the slow frequency on the particle energy. A positive shift of the ω_z frequency, as compared to the frequency predicted by equation (21), is reported, also.

To this goal, equation (13) has been integrated using different values of the ϵ parameter, in the range 0 to 0.17. In all integrated motions, the particle was released at a given ζ , with zero velocity, and at the angular phase $\tau = 0$ of the driving field. Apparently, these initial conditions are not sufficient for a complete analysis. But a more detailed study [10], shows that in the main stability domain which is positioned near the bottom of the effective potential, these initial conditions allow an efficient exploration of the region. For the sake of simplicity, we chose to sort the maximum values of the velocity $\zeta_{\max} = (d\zeta/d\tau)_{\max}$, which are in direct relation with the maximum kinetic energy of the particle, and it is a good parameter for displaying most of the curves involved here. In order to derive the amplitude of the motion, the extrema ζ_{\min} and ζ_{\max} were sorted also.

Notice that the invariants we verified refer to the slow motion that is only part of the total motion, the other one being the fast component. Their numerical separation proves to be very fruitful in deriving the results of this section.

To avoid some possible confusion, also notice that all the results in this section were derived from the numeric integration of equation (13) only.

We did not attempt to integrate equation (14). We have only speculated its properties.

The $\mathcal{A}\mathcal{T}$ invariant. For motions of low amplitude, where the adiabatic approximation works well, one can expect that the numerical value provided by equation (15) will be retrieved again. At this point, another problem arose: How to compute the quantities \mathcal{A} and \mathcal{T} from the available data? To this goal, two numerical algorithms have been developed: one for the amplitude, and the second one for the frequency of the slow motion.

Particularly, the algorithm for the amplitude allows a fair estimation of the limits Z_{\min} and Z_{\max} of the slow motion. Concerning the calculation of the frequency of the slow motion, we have developed an algorithm described in [10].

The numerical results show that for $c = 0$

$$\mathcal{A}\mathcal{T} = 7.41028 - 11.4812 Z_{\max}^2 \quad (22)$$

The first term on the right hand of above relation is close enough to the value predicted by equation (17). The discrepancy comes from the following known facts: (a) the better the frequency estimation, the longer the time of measurement as compared to the period of implicated motion; (b) the longer the time of integration, the larger the numeric errors; (c) accordingly to equation (17) that works in the adiabatic approximation, low amplitudes imply high periods of the slow motion. This way, the time of integration was chosen at the end of an optimal decision.

Maximum elongations. The maximum elongations ζ_{\min} and ζ_{\max} are easily sorted using the integrated trajectories. Fig. 2 displays their dependence on $(d\zeta/d\tau)_{\max}$. As for the elongation, Z_{\min} and Z_{\max} were computed using the amplitude algorithm aforementioned.

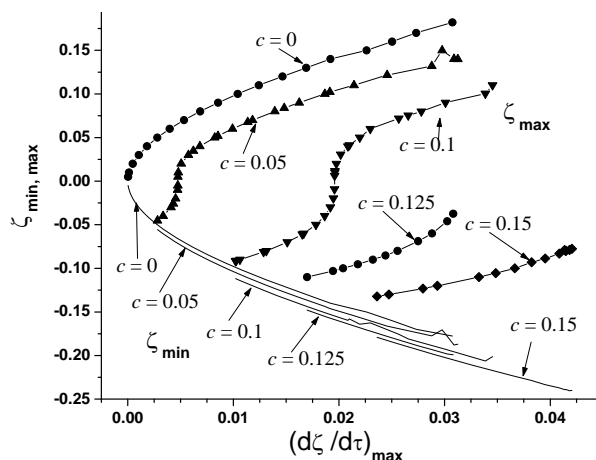


Fig. 2. Dependence of ζ_{\min} and ζ_{\max} versus $(d\zeta/d\tau)_{\max}$ for some values of the c parameter. The solid lines represent the lower limit, while the dotted ones are for the upper limit.

Fig. 2 reveals a common particularity of these functions: in the vicinity of some point, every motion takes the smallest value of the amplitude. Surprisingly, as motions with $c = 0.15$ prove it, near this minimum there are stable motions at large values of the kinetic energy as compared to the $c = 0$ case.

The numerical analysis shows that the maximum elongations of the slow motion Z_{\min} and Z_{\max} are related to the maximum elongations ζ_{\min} and ζ_{\max} by the smooth functions given below. Concerning ζ_{\min} , the $c = 0$ case looks like an accident case, and has been separately treated, while, for ζ_{\max} , the case $v = 0.15$ has been treated likewise.

1. For $c = 0$:

$$\zeta_{\min} = 0.97848 Z_{\min} - 1.41493 Z_{\min}^2.$$

2. For $0.025 \leq c \leq 0.15$:

$$\zeta_{\min} = (0.00742 - 0.08882c + 1.88818c^2) + (1.18941 + 0.41497c + 8.74248c^2) Z_{\min}^2.$$

3. For $0 \leq c \leq 0.125$:

$$\zeta_{\max} = (-2.0718 \cdot 10^{-2} - 0.00809c) + (0.78409 + 0.18096c) Z_{\max}^2 + (1.4824 - 4.80688c) Z_{\max}^3.$$

4. For $v = 0.15$:

$$\zeta_{\max} = 0.00748 + 1.12947 Z_{\max}^2 + 1.44886 Z_{\max}^3.$$

The residual motion. The numeric analysis focuses now on the zones of smallest amplitude. At the bottom of the effective potential function, the motion of the particle contains only the fast motion, this kind of motion is referred to as *residual motion*. At this limit, both Z_{\min} and Z_{\max} take a common value Z_c . This value represents the true position of the minimum of the effective potential function Z_c could be expressed in terms of v as

$$Z_c = -0.89881c - 0.60444c^2 - 1.09074c^3 - 0.49474c^4, \quad (23)$$

while the slow frequency is given by

$$\omega_s = c + 0.14108c^2 + 0.74782c^3 + 16.081c^4. \quad (24)$$

All these formulae agree well with the available data in 1% in the range of c from 0 to 0.17.

The energetic invariant. If the $2\mathcal{H}$ invariant exists then it is possible to compute Z_{\max} from a function like $g(Z, c) = \sqrt{f(Z) + c^4/6}$, where $f(c) = c^2/2 + 2c^3/3$.

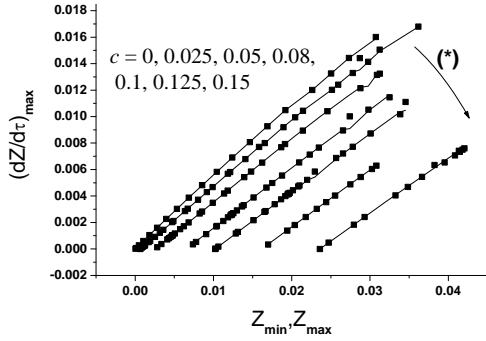


Fig. 3. Plots of the \max and \min functions versus, x at seven values of c : 0, 0.025, 0.05, 0.08, 0.1, 0.125, and 0.15. The function \max is represented with solid lines, while the squared symbols belong to \min . The arrow marked with (*) indicates the direction in which c increases.

In order to verify both the existence of the $2H$ invariant and to establish a method for computing Z_{\max} , the functions $g(Z_{\min}, -Z_c)$ and $g(Z_{\max}, -Z_c)$ were represented on the same plot for a couple of c values. The idea of substituting c with $-Z_c$ proves to be excellent, since all the graphics of $g(Z_{\min}, -Z_c)$ and $g(Z_{\max}, -Z_c)$ in Fig. 3 come close together for all values of c .

The excellent overlapping of the two functions demonstrates the existence of an energetic invariant of the following form

$$Z^2 + \frac{p_z^2}{2} - \frac{16Zp_z^2}{9} = \text{constant} = 2H \quad (25)$$

where Z_c represents the position of the minimum of the effective potential given by equation (23). The discrepancy between (18) and (25) becomes important for large values of c in the studied range.

Due to the excellent verification of the energetic invariant (25), the formula

$$Z_{\max} = g(Z_{\min}, -Z_c) \quad (26)$$

was used when constructing the plots in Fig. 3. It qualifies as a good formula for Z_{\max} that otherwise would be difficult to estimate.

The slow frequency. As opposed to the $c = 0$ case, for $c \neq 0$ the frequency ω_s has a nonmonotonic dependence on $Z_{\max} = (dZ/dt)_{\max}$, as Fig. 4 shows.

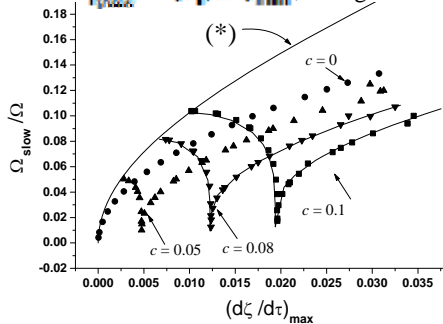


Fig. 4. Dependence of the slow frequency versus $(dZ/dt)_{\max}$. The curved line marked with asterisk (*) represents the limit of all such dependencies. In its points, the ion experiences only residual motion.

The values of the dotted function in Fig. 4 have been computed using the aforementioned frequency algorithm. The two V-shaped lines from the same figure are calculated functions using the formula

$$\omega_s = 2n(1 + 0.23c)/T, \quad (27)$$

where the value of T resulted from equation (21).

Near such a minimum (of a V-shaped line), the ion is moving towards $\dot{\varphi} = 0$ with very slow velocity. Such motions show a pronounced chaotic dynamics.

There were some difficulties in calculating the improper integral in equation (21), but we do not believe that they affected the observed positive shift.

6. Motion stability for 3D motions.

In order to take into account the effect of the centrifugal force, we have considered the dimensionless Hamiltonian in cylindrical coordinates for a single charged particle moving into a hexapole trap

$$H = (p_r^2 + p_z^2 + p_\varphi^2/u^2)/2 + (c + \cos\varphi)(2v^2 - 8uv^2)/\theta \quad (28)$$

that yields to the equations of motion

$$\begin{aligned} d^2u/dt^2 &= (c + \cos\varphi)(uv + p_\varphi^2/u^3), \\ d^2v/dt^2 &= (c + \cos\varphi)(u^2/2 + v^2), \\ d\varphi/dt &= p_\varphi/u^2, \end{aligned} \quad (29)$$

where the dimensionless spatial coordinates are related to the usual cylindrical coordinates (r, u, φ) by $[u, v] = (8/9)q_c[r, z]/z_p$, the time scale being $\tau = \Omega_c$, and $p_\varphi = 9M_e/(16m\Omega_c z_p)$. In the last relation, M_e is the angular momentum of the particle with respect to the z -axis.

The dynamic and static potential functions are now

$$\begin{aligned} \Psi_c(R, Z) &= (Z^4/4 + R^4/16 + p_\varphi^2/2R^2), \\ \Psi_s(R, Z) &= c(2Z^2 - 8ZR^2)/\theta. \end{aligned} \quad (30)$$

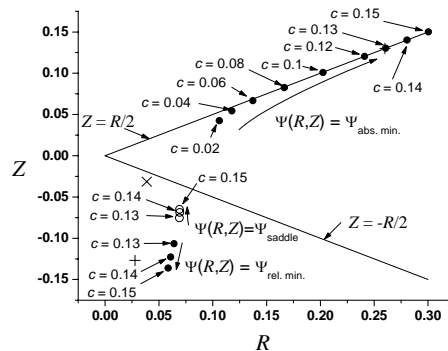


Fig. 5. The position of the extrema of the effective potential function. The full circle corresponds to the minimum points and the hollow circle to saddle points in the case. The cross (+) corresponds to the minimum points and the cross (x) to the saddle point when, and.

In the new circumstances, the effective potential function $\Psi(R, Z, p_\phi, c) = \Psi_z(R, Z, p_\phi) + \Psi_r(R, Z, c)$ has two parameters: p_ϕ and c . As before, we looked for the extrema of the effective potential function. As expected, in this case the relative minimum belonging to the z-axis disappears. Also foreseeable, for low values of c , an absolute minim exists near the $Z = R/2$ line as Fig. 5 shows.

Surprisingly, starting at some value of c depending on the p_ϕ parameter, a relative minimum appears positioned in the opposite side of the $Z = 0$ plane, as near the z-axis as the first one. For instance, at $p_\phi = 0.0003$, the relative minimum appears for values of c greater than 0.12 approximately.

Figure 5 shows the location of the extrema in the effective potential for two values of the p_ϕ at various values of the c parameter. So, if we chose for instance $p_\phi = 0.0003$, and $c = 0.13$, the function would have an absolute minimum at $(R = 0.26009, Z = 0.13028)$, a relative minimum at $(R = 0.06408, Z = -0.1068)$, and a saddle point at $(R = 0.06908, Z = -0.0738)$.

The plot in Fig. 5 reveals that for $c \leq 0.12$ the Ψ function has only one absolute minimum near the $Z = R/2$ line.

If, for instance, in the numeric integration of the system (28), we chose for the initial position of the particle the minimum of the effective potential function, $p_\phi = 0.0003$, and $c = 0.13$, long-term bounded trajectories are obtained (see Fig. 6). This proves that these points belong to the stability domain of the hexapole trap

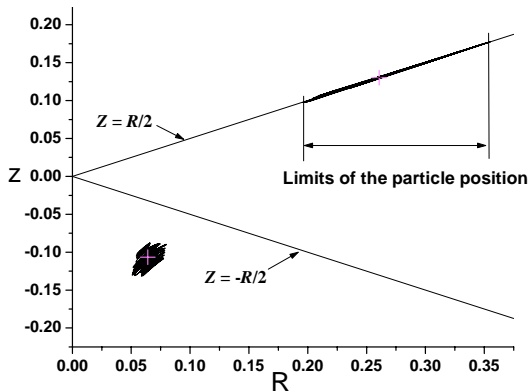


Fig. 6. Stable particle trajectories near the bottom of the effective potential function. The particle was launched from the bottom of the effective potential function with $p_\phi = 0.0003$, and $c = 0.13$.

Fig. 6 shows that for the upper motion (near the absolute minimum of the effective potential function) extends almost along the $Z = R/2$ line.

On the contrary, for the lower trajectory (near the relative minimum) extends over comparable domains in both directions r and z . The two light-gray cross marks indicate the position of the minimum of the effective

potential function from where the particle was launched in the simulation.

7. Conclusions

The motion stability in a hexapole rf trap under non null DC component was investigated. Generally, as for the octupole rf trap, the presence of a DC component weakens the motion stability in the hexapole rf trap.

Mainly, two objectives were pursued in this analysis: (i) to find if, and under what conditions, stable motions are possible; (ii) what are the reasons for weakening the motion stability under non-zero DC component.

Concerning the first question, we looked for the minima of the effective potential where we assumed that stable motions are possible. As the dedicated section proved, the answer is clearly yes for rectilinear motions. Also, the above assumption proves to be true for both 2D and 3D motions, as the numerical results show.

The good agreement between theory and the numeric results for 1D motions has its two-fold importance: (a) it validates the theory of the effective potential, and (b) it attests the accuracy of the numeric methods used.

As for the discrepancies, there should be a better theory that expects to be discovered.

In the numerical analysis of the 2D motions, long-term bounded motions were recorded in the vicinity of the minima of the effective potential. Unlike the null DC component case, a particle launched near the bottom of the effective potential exhibits a residual motion whose amplitude increases with c . Also, since it is a minimax for the effective potential function, the origin is not a stable equilibrium point for the rf hexapole trap. Moreover, the motions in which the ion approaches the trap center with very low velocity exhibit chaotic dynamics. In the case of rectilinear motions: the closer the limit of the trajectory to the trap center, the closer to zero the frequency of the slow motion.

Regarding the 3D case, the effective potential function allows to consider the stability of motions with non null angular momentum with respect to the z-axis. As expected in such cases, the bottom of the effective potential function does not belong to the symmetry axis. Besides, it is found that, for relatively large values of c , the spatial stability domain is divided into two parts: one having the center near the cone $Z = R/2$ and another, on the opposite side of the $Z = 0$ plane, and closer to the symmetry axis than the first one.

As for the answer to the second question, we found that the deterioration of the motion stability is mainly produced by shifting the motion to spatial locations where the intensity of the driving field is larger. In these regions, even a small perturbation could become decisive. Also, the presence of multiple minima of the effective potential introduces more slow frequencies, and, consequently, more chances for the trapping environment to induce resonance phenomena on the particle motion. Even when these frequencies do not have the exact value of some slow frequency, when they are close enough, the resonance

phenomena take place increasing the kinetic energy of the particle.

The theory predicted all the major features of the motion studied, but fails in giving the exact position of the minima of the effective potential (23), and the exact value of the frequency of the slow motion (26). Both observed shifts increase with σ . Unlike the $\sigma = 0$ case, for $\sigma \neq 0$ the shift of ω_s increases with the kinetic energy also (22).

Due to these observations, we may conclude that under DC component the validity of the adiabatic theory extends much further than for the null DC case.

In contrast to the quadrupole (Paul) trap for nonlinear rf traps of higher order (hexapole, octupole, and so on) the frequency of the slow motion depends on the kinetic energy of the particle. Moreover, the number of slow frequencies increases with the order of the trap.

As compared to the octupole trap, the DC component seems to have a smaller influence on the stability of the hexapole rf trap.

References

- [1] W. Paul, Rev. Mod. Phys. **62**, 531 (1990).
 [2] F. M. Penning, Physica **3**, 873 (1936).
 [3] J. Walz, I. Siemers, M. Schubert, W. Neuhauser, R. Blatt, E. Teyl, Phys. Rev. A **50**, 4122 (1994).
 [4] C. M. Niculae, Europhys. Lett. **43**, 398 (1998).
 [5] E. C. Beaty, Phys. Rev. A **33**, 3645 (1986).
 [6] R. Takai, K. Nakayama, W. Saiki, K. Ito, H. Okamoto, J. Phys. Soc. Jpn. **76**, 014802 (2007).
 [7] I. Siemers, M. Schubert, R. Blatt, W. Neuhauser, P. E. Toschek, Europhys. Lett. **18**, 129 (1992).
 [8] H. G. Dehmelt, Adv. At. Mol. Phys. **3**, 53 (1967).
 [9] P. L. Kapitsa, Zh. Experm. i. Teor. Fiz. **21**, 588 (1951).
 [10] C. M. Niculae, Europhys. Lett. **77**, 50001 (2007).
 [11] L. D. Landau, E. M. Lifshitz, Mechanics, Pergamon Press, 1976.
 [12] C. M. Niculae, Rom. Rep. in Phys. **50**, 665 (1998).
 [13] C. M. Niculae, Acta Phys. Polonica A **98**, 719 (1998).

*Corresponding author: cniculae@gmail.com